

doi: 10.12029/gc20210212

王金芳,李英杰,李红阳,董培培. 2021. 二连—贺根山缝合带晚石炭世埃达克岩的发现及古亚洲洋洋内俯冲作用[J]. 中国地质, 48(2): 520–535.

Wang Jinfang, Li Yingjie, Li Hongyang, Dong Peipei. 2021. Discovery of the Late Carboniferous adakite in the Erenhot–Hegenshan suture zone and intra-oceanic subduction of the Paleo-Asian Ocean [J]. *Geology in China*, 48(2):520–535(in Chinese with English abstract).

## 二连—贺根山缝合带晚石炭世埃达克岩的发现 及古亚洲洋洋内俯冲作用

王金芳,李英杰,李红阳,董培培

(河北地质大学地球科学学院,河北 石家庄 050031)

**摘要:**内蒙古二连—贺根山缝合带额很傲包图英云闪长岩体, 出露于西乌旗梅劳特乌拉 SSZ 型蛇绿岩带北侧。为了确定该岩体的岩石成因类型, 探讨其构造环境及古亚洲洋俯冲消亡过程, 对该岩体进行了岩石学、地球化学和 LA-ICP-MS 锆石 U-Pb 年代学研究。额很傲包图英云闪长岩高硅富铝, 富钠贫钾, 高铯低钇, 富集 Rb、Ba、Sr 等大离子亲石元素和 LREE, 亏损 Nb、Ta、Ti、P 等高场强元素和 HREE, 无明显 Eu 异常。岩石学和岩石地球化学特征表明, 该英云闪长岩体为高 Si 埃达克岩(HSA), 形成于岛弧环境, 具有洋内俯冲洋壳+俯冲深积物部分熔融并与上覆地幔楔橄榄岩反应成因特征。锆石 LA-ICP-MS U-Pb 测年表明, 额很傲包图英云闪长岩体的侵位年龄为(305.6 ± 1.5)Ma, 形成时代为晚石炭世。结合二连—贺根山缝合带石炭纪蛇绿岩、石炭纪—二叠纪岛弧型岩浆岩的时空分布与演化特征, 认为古亚洲洋二连—贺根山洋盆在石炭纪—早二叠世处于以洋内俯冲为特征的大洋俯冲消亡过程中。

**关键词:**英云闪长岩;埃达克岩;洋内俯冲作用;晚石炭世;二连—贺根山缝合带;地质调查工程

**中图分类号:**P588.12<sup>2</sup>;P597<sup>3</sup>;P595 **文献标志码:**A **文章编号:**1000-3657(2021)02-0520-16

## Discovery of the Late Carboniferous adakite in the Erenhot–Hegenshan suture zone and intra-oceanic subduction of the Paleo-Asian Ocean

WANG Jinfang, LI Yingjie, LI Hongyang, DONG Peipei

(College of Earth Sciences, Hebei GeoUniversity, Shijiazhuang, 050031, Hebei, China)

**Abstract:** The Ehenaoabaotu tonalite is outcropped in the northern part of the Meilaotewula SSZ-type ophiolite of the Erenhot–Hegenshan suture zone in Xi Ujimqin Banner of Inner Mongolia. Based on the study of petrology, geochemistry and zircon LA-ICP-MS U-Pb geochronology, the genetic type and tectonic setting of the tonalite were determined, and the final closure time and subduction process of the Erenhot–Hegenshan ocean basin of the Paleo-Asian Ocean were discussed. The tonalite is characterized by high SiO<sub>2</sub>, Al<sub>2</sub>O<sub>3</sub>, Na<sub>2</sub>O, Sr and low K<sub>2</sub>O, Y contents, enrichment of Rb, Ba, Sr large ion lithophile elements and LREE, and depletion of Nb, Ta, Ti, P high field strength elements and HREE. There is no pronounced Eu anomaly. The lithological and

收稿日期:2018-05-08;改回日期:2020-07-02

基金项目:国家自然科学基金“内蒙古迪彦庙蛇绿岩带前弧玄武岩组合及其成因”(41972061)和中国地质调查局“内蒙古1:5万高力罕牧场三连等四幅区调”(1212011120711)、“内蒙古1:5万沙日勒昭等四幅区调”(1212011120701)项目联合资助。

作者简介:王金芳,女,1983年生,副教授,从事岩石学和地球化学研究;E-mail: wjfb1983@163.com。

geochemical characteristics show that the Ehenaoaotu pluton is a high Si adakite (HSA) formed in island arc, and was derived from partial melting of the intra-oceanic subducting oceanic crust and sediment and subsequently reaction with overlying mantle wedge peridotite. Its U-Pb LA-ICP-MS dating yields  $(305.6 \pm 1.5)$  Ma and suggests that the Ehenaoaotu pluton was formed during Late Carboniferous. Combined with the study of spatio-temporal evolution of the Carboniferous ophiolites and Carboniferous-Permian island arc magmatic rocks in the Erenhot-Hegenshan suture, it is assumed that the Erenhot-Hegenshan oceanic basin of the Paleo-Asian Ocean was in the process of oceanic subduction characterized by intra-oceanic subduction during the Carboniferous-Early Permian.

**Key words:** tonalite; adakite; intra-oceanic subduction; Late Carboniferous; Erenhot-Hegenshan suture zone; geological survey engineering

**About the first author:** WANG Jinfang, female, born in 1983, associate professor, engaged in the study of petrology and geochemistry.

**Fund support:** Funded by National Natural Science Foundation of China (No.41972061) and the projects of China Geological Survey(No.1212011120711, No.1212011120701).

## 1 引言

中亚造山带东段二连—贺根山缝合带是华北板块与西伯利亚板块的重要缝合界线之一,蕴涵着古亚洲洋二连—贺根山洋盆的俯冲消亡过程与信息(Xiao et al., 2003; Windley et al., 2007; Zhang et al., 2015; 邓晋福等, 2015; 李钢柱等, 2017)。内蒙古中部西乌旗地区为二连—贺根山缝合带古生代蛇绿岩和岛弧岩浆岩的典型发育地区之一,识别与研究这些古生代岛弧岩浆岩与蛇绿岩之间的时空分布关系和内在成因联系,对了解古亚洲洋二连—贺根山洋盆闭合时间和大洋俯冲消亡过程具有重要意义(陈斌等, 2001; Miao et al., 2008; 刘建峰等, 2009; 李英杰等, 2012, 2018b; Liu et al., 2013; 董培培等, 2020)。然而,二连—贺根山洋盆闭合时间仍存在着“晚泥盆世”与“晚二叠世”较大分歧(Shang, 2004; Miao et al., 2008; Xiao et al., 2009; 邵济安, 2015; 田树刚等, 2016),与该区晚古生代石炭纪蛇绿岩密切伴生的晚石炭世岛弧型埃达克岩体也尚未见有报道,二连—贺根山洋盆“晚二叠世”闭合时间仍需要进一步的岩石学证据与年代学约束。笔者近年在内蒙古1:5万高力罕牧场三连等四幅区域地质矿产调查中,新识别出额很傲包图英云闪长岩体。1:20万罕乌拉幅区域地质矿产调查将该岩体划归为华力西晚期石英闪长岩,缺少地球化学和年代学等资料。因此,本文在1:5万区域地质调查的基础上,选择西乌旗梅劳特乌拉SSZ型蛇绿岩北侧出露的额很傲包图英云闪长岩(图1)进行岩石学、地球化学和年代学研究,探讨其岩石成因类型及形成的构造环境,以期

为古亚洲洋二连—贺根山洋盆俯冲消亡时间与过程提供一些岩石学、地球化学和年代学证据和约束。

## 2 区域地质背景和岩石学特征

研究区位于内蒙古西乌旗东北部,大地构造位置处于华北板块北缘增生带与西伯利亚板块南缘增生带的碰撞缝合部位,属于中亚造山带东段的二连—贺根山缝合带(图1a)。额很傲包图英云闪长岩体出露于梅劳特乌拉SSZ型蛇绿岩北侧(图1b)(李英杰等, 2015; 王金芳等, 2017a, 2018c),侵入于晚石炭世花岗岩之中,被早白垩世正长花岗岩所侵入(王金芳等, 2017b),出露面积约27 km<sup>2</sup>(图1b, c)。额很傲包图英云闪长岩呈浅灰色、浅灰绿色和灰白色,中粒—粗中粒半自形粒状结构,块状构造(图1d, e),矿物成分主要为斜长石(45%~55%)、石英(30%~35%)、黑云母(8%~10%)和角闪石(3%~5%),少量钾长石(2%±)。斜长石自形—半自形板状,可见卡钠复合双晶,双晶纹中细,部分颗粒具环带构造,偶见净边结构,均已不同程度绢云母化;石英它形粒状,部分颗粒可见波状消光;黑云母多为自形片状,可见绿泥石化;角闪石呈半自形柱状,可见黝帘石化和绿泥石化。

## 3 锆石U-Pb年代学

本文在额很傲包图采集了1件新鲜的英云闪长岩年龄样品(PS1-10),采样点地理位置:45°02′25.6″N、118°27′42.0″E(图1b, c)。

样品PS1-10的锆石挑选由河北省区域地质矿产调查研究所实验室完成。将岩石样品破碎成粉

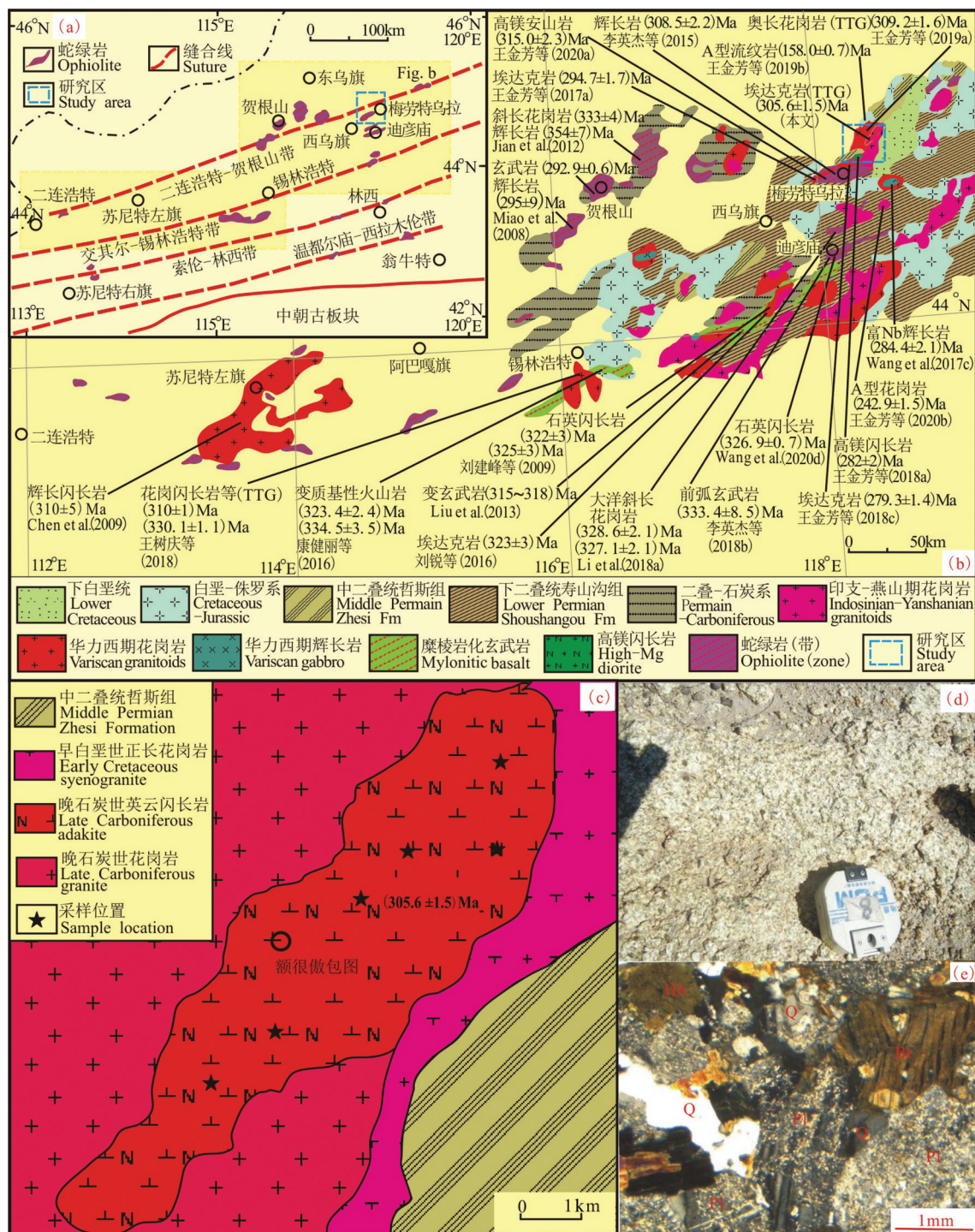


图1 额很傲包图英云闪长岩大地构造单元图(a)(修改自 Miao et al., 2008),区域地质图(b),地质图(c),野外照片(d)和显微照片(e)  
Fig.1 Tectonic unit map (a)(modified from Miao et al., 2008), regional geological map (b), geological map(c), field photograph (d) and photomicrograph (e) of the Ehenaboauto tonalite

末,利用重液和磁选法分离技术分选。此后,在双目镜下根据晶形的完好程度、颜色的有无、透明度的高低以及包裹体和裂纹的有无等挑选出测试的锆石,然后用环氧树脂在玻璃板上固定挑选好的锆

石与标样抛光至锆石中心(制靶)。通过双目镜和阴极发光(CL)图像研究锆石的晶形和内部结构,选择原位同位素分析的最佳点。制靶和阴极发光实验在北京锆年领航科技有限公司完成,锆石原位

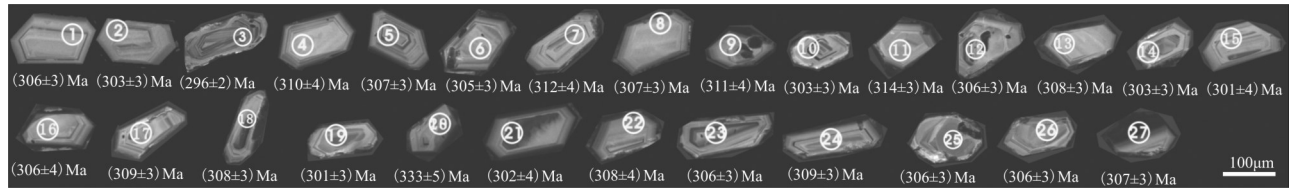


图2 额很傲包图英云闪长岩(PS1-10)锆石阴极发光图像及其LA-ICP-MS U-Pb年龄

Fig.2 Cathodoluminescent images and LA-ICP-MS U-Pb ages of zircons from the Ehenaoaotu tonalite

U-Pb同位素年龄在天津地质调查中心激光剥蚀等  
离子体质谱仪(LA-ICP-MS)上测定。进行了锆石  
样品测试数据的普通铅校正处理、U-Pb年龄谐和  
图的绘制和年龄权重平均计算(Ludwig, 2003)。

测试样品锆石无色透明,呈自形柱状或双锥  
状,长短轴之比为1:1~2:1,几乎所有27颗锆石均显  
示较为典型的岩浆韵律振荡环带(图2),表明这些锆  
石为酸性岩浆成因。测试结果Th、U含量和Th/U比  
值分别为  $59 \times 10^{-6}$ ~ $331 \times 10^{-6}$ 、 $3 \times 10^{-6}$ ~ $18 \times 10^{-6}$  和

0.0628~0.8842,反映了岩浆成因的特征(Corfu et  
al., 2003; Wu et al., 2004)。27粒锆石的测定年龄值  
均落在谐和线上或附近,其 $^{206}\text{Pb}/^{238}\text{U}$ 年龄加权平均  
值为 $(305.6 \pm 1.5)\text{Ma}$ (MSWD=1),代表该英云闪长  
岩的侵位结晶年龄(表1,图3)。

## 4 地球化学特征

### 4.1 主量元素特征

研究区6件地球化学样品的主量和微量元素测

表1 额很傲包图英云闪长岩(PS1-10)LA-ICP-MS 锆石U-Pb测试结果  
Table 1 LA-ICP-MS U-Pb dating of zircons from the Ehenaoaotu tonalite

| 点号 | 含量/ $10^{-6}$ |     | Th/U   | 同位素比值                                 |         |                                    |         |                                    |         | 表面年龄/Ma                            |         |
|----|---------------|-----|--------|---------------------------------------|---------|------------------------------------|---------|------------------------------------|---------|------------------------------------|---------|
|    | Pb            | U   |        | $^{207}\text{Pb}^*/^{206}\text{Pb}^*$ | $\pm\%$ | $^{207}\text{Pb}^*/^{235}\text{U}$ | $\pm\%$ | $^{206}\text{Pb}^*/^{238}\text{U}$ | $\pm\%$ | $^{206}\text{Pb}^*/^{238}\text{U}$ | $\pm\%$ |
| 1  | 6             | 122 | 0.3858 | 0.0663                                | 7.01    | 0.4445                             | 7.08    | 0.0486                             | 0.93    | 306                                | $\pm 3$ |
| 2  | 15            | 286 | 0.6116 | 0.0555                                | 5.71    | 0.3686                             | 5.79    | 0.0482                             | 0.89    | 303                                | $\pm 3$ |
| 3  | 11            | 215 | 0.5546 | 0.0551                                | 5.10    | 0.3574                             | 5.16    | 0.0470                             | 0.83    | 296                                | $\pm 2$ |
| 4  | 6             | 108 | 0.4663 | 0.0547                                | 18.78   | 0.3709                             | 18.0    | 0.0492                             | 1.15    | 310                                | $\pm 4$ |
| 5  | 11            | 206 | 0.5115 | 0.0528                                | 5.30    | 0.3553                             | 5.39    | 0.0488                             | 0.83    | 307                                | $\pm 3$ |
| 6  | 6             | 124 | 0.3639 | 0.0561                                | 8.31    | 0.3752                             | 8.15    | 0.0485                             | 1.01    | 305                                | $\pm 3$ |
| 7  | 4             | 83  | 0.4065 | 0.0616                                | 11.43   | 0.4217                             | 10.9    | 0.0496                             | 1.13    | 312                                | $\pm 4$ |
| 8  | 13            | 259 | 0.3904 | 0.0601                                | 5.82    | 0.4045                             | 5.83    | 0.0488                             | 0.87    | 307                                | $\pm 3$ |
| 9  | 6             | 110 | 0.2835 | 0.0517                                | 25.98   | 0.3524                             | 25.1    | 0.0495                             | 1.43    | 311                                | $\pm 4$ |
| 10 | 12            | 225 | 0.5785 | 0.0550                                | 5.42    | 0.3644                             | 5.59    | 0.0481                             | 0.86    | 303                                | $\pm 3$ |
| 11 | 7             | 136 | 0.4376 | 0.0523                                | 9.64    | 0.3591                             | 9.70    | 0.0498                             | 1.03    | 314                                | $\pm 3$ |
| 12 | 9             | 176 | 0.4280 | 0.0519                                | 6.35    | 0.3471                             | 6.41    | 0.0485                             | 0.85    | 306                                | $\pm 3$ |
| 13 | 6             | 122 | 0.3991 | 0.0560                                | 9.18    | 0.3780                             | 9.18    | 0.0489                             | 0.97    | 308                                | $\pm 3$ |
| 14 | 11            | 218 | 0.4720 | 0.0541                                | 5.48    | 0.3589                             | 5.61    | 0.0481                             | 0.84    | 303                                | $\pm 3$ |
| 15 | 4             | 84  | 0.4081 | 0.0536                                | 19.13   | 0.3530                             | 17.5    | 0.0478                             | 1.37    | 301                                | $\pm 4$ |
| 16 | 3             | 59  | 0.4794 | 0.0868                                | 13.64   | 0.5807                             | 12.5    | 0.0485                             | 1.40    | 306                                | $\pm 4$ |
| 17 | 4             | 87  | 0.4436 | 0.0749                                | 9.16    | 0.5073                             | 9.01    | 0.0491                             | 1.11    | 309                                | $\pm 3$ |
| 18 | 18            | 331 | 0.8842 | 0.0512                                | 3.68    | 0.3439                             | 3.83    | 0.0487                             | 0.89    | 307                                | $\pm 3$ |
| 19 | 9             | 206 | 0.0628 | 0.0537                                | 5.83    | 0.3538                             | 5.94    | 0.0478                             | 0.85    | 301                                | $\pm 3$ |
| 20 | 3             | 60  | 0.5249 | 0.0492                                | 43.97   | 0.3598                             | 30.0    | 0.0530                             | 1.40    | 333                                | $\pm 5$ |
| 21 | 4             | 84  | 0.4270 | 0.0612                                | 15.19   | 0.4051                             | 14.8    | 0.0480                             | 1.33    | 302                                | $\pm 4$ |
| 22 | 4             | 82  | 0.4161 | 0.0819                                | 9.56    | 0.5519                             | 9.65    | 0.0489                             | 1.34    | 308                                | $\pm 4$ |
| 23 | 10            | 193 | 0.6232 | 0.0518                                | 5.80    | 0.3471                             | 5.85    | 0.0486                             | 0.85    | 306                                | $\pm 3$ |
| 24 | 7             | 127 | 0.4639 | 0.0754                                | 5.94    | 0.5106                             | 6.09    | 0.0491                             | 0.97    | 309                                | $\pm 3$ |
| 25 | 5             | 104 | 0.2562 | 0.0528                                | 14.44   | 0.3538                             | 14.0    | 0.0486                             | 1.09    | 306                                | $\pm 3$ |
| 26 | 5             | 94  | 0.3005 | 0.0617                                | 9.65    | 0.4142                             | 9.45    | 0.0487                             | 1.07    | 306                                | $\pm 3$ |
| 27 | 7             | 133 | 0.3657 | 0.0581                                | 7.40    | 0.3913                             | 7.41    | 0.0488                             | 0.89    | 307                                | $\pm 3$ |

注:误差为  $1\sigma$ ; Pb\* 指示放射成因铅; 实验测试在天津地质矿产研究所完成。

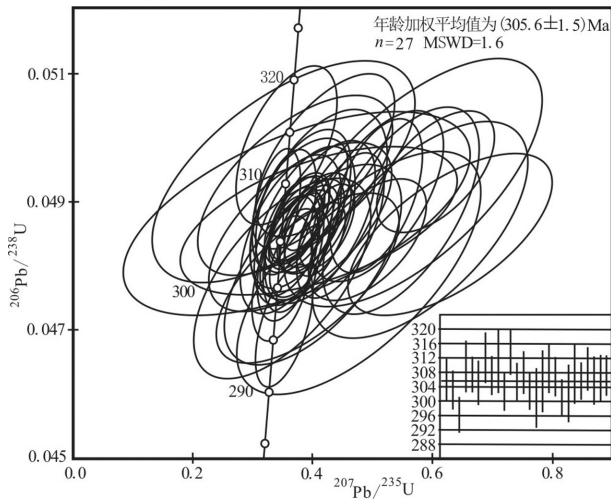


图3 额很傲包图英云闪长岩(PS1-10)锆石 LA-ICP-MS U-Pb 年龄谱和图和直方图

Fig.3 U-Pb concordia diagram and histograms of zircons from the Ehenaoabaotu tonalite

试分析均在河北省区域地质矿产调查研究所实验室完成,主量元素分析采用 Axios<sup>max</sup> X 射线荧光光谱仪测定,精度在 1% 以内,微量元素和稀土元素采用 X Series 2 等离子体质谱仪测定,测试精度在 5% 以内。主量、微量和稀土元素测试分析数据列于表 2。

从表 2 可知,额很傲包图英云闪长岩 SiO<sub>2</sub> 含量为 65.97%~67.92%, 平均值 66.55%; Al<sub>2</sub>O<sub>3</sub> 含量 15.57%~16.36%, 平均值 16.04%, 总体表现出高硅富铝特征; 岩石 Na<sub>2</sub>O 含量为 4.25%~5.22%, K<sub>2</sub>O 含量为 1.67%~1.95%, Na<sub>2</sub>O/K<sub>2</sub>O 比值为 2.23~2.98, 显示富钠贫钾; 全碱 (Na<sub>2</sub>O+K<sub>2</sub>O) 含量为 6.10%~6.97%, 平均值 6.36%; 里特曼指数 σ 为 1.59~1.94, 平均值 1.72, 为钙碱性岩; MgO 含量 1.19%~1.98%, Mg<sup>#</sup>42~51, 平均值 47; 相对贫 TiO<sub>2</sub> (0.46%~0.51%) 和 P<sub>2</sub>O<sub>5</sub> (0.149%~0.161%)。该岩石的铝饱和指数 A/CNK 值介于 1.02~1.18, A/NK 为 1.56~1.80, 属弱过铝质—强过铝质(图 4)。在 SiO<sub>2</sub>-(Na<sub>2</sub>O+K<sub>2</sub>O)(TAS) 分类图解中, 样品落入亚碱性花岗岩闪长岩区域(图 5)。在 An-Ab-Or 图解中除 1 件样品落入奥长花岗岩区外, 其余 5 件样品均落入英云闪长岩区(图 6)。

4.2 稀土元素特征

额很傲包图英云闪长岩的稀土元素含量如表 2 所示, ΣREE 变化范围为 53.01×10<sup>-6</sup>~80.93×10<sup>-6</sup>, 平均值 62.68×10<sup>-6</sup>, 相对较低; Yb 含量 0.82×10<sup>-6</sup>~1.33×

表 2 额很傲包图英云闪长岩主量(%),微量和稀土(10<sup>-6</sup>)元素分析结果

Table 2 Major element(%), trace element and REE analyses (10<sup>-6</sup>) of the Ehenaoabaotu tonalite

| 样号                             | PS1-08 | PS1-09 | PS1-10 | PS1-11 | PS1-12 | PS1-13 | 高Si埃达克岩 |
|--------------------------------|--------|--------|--------|--------|--------|--------|---------|
| SiO <sub>2</sub>               | 66.58  | 66.45  | 66.03  | 67.92  | 66.37  | 65.97  | 64.8    |
| TiO <sub>2</sub>               | 0.50   | 0.49   | 0.48   | 0.48   | 0.46   | 0.51   | 0.56    |
| Al <sub>2</sub> O <sub>3</sub> | 15.57  | 16.14  | 15.84  | 16.33  | 16.36  | 15.98  | 16.64   |
| Fe <sub>2</sub> O <sub>3</sub> | 2.05   | 1.99   | 1.84   | 1.87   | 1.90   | 1.94   | 4.75    |
| FeO                            | 1.63   | 1.55   | 1.75   | 1.27   | 1.60   | 1.83   |         |
| MnO                            | 0.071  | 0.071  | 0.072  | 0.053  | 0.064  | 0.066  | 0.081   |
| MgO                            | 1.64   | 1.94   | 1.68   | 1.19   | 1.49   | 1.98   | 2.18    |
| CaO                            | 3.39   | 2.90   | 3.33   | 1.84   | 3.55   | 2.98   | 4.63    |
| Na <sub>2</sub> O              | 4.25   | 4.45   | 4.46   | 5.22   | 4.43   | 4.46   | 4.19    |
| K <sub>2</sub> O               | 1.91   | 1.81   | 1.95   | 1.75   | 1.67   | 1.82   | 1.97    |
| P <sub>2</sub> O <sub>5</sub>  | 0.151  | 0.157  | 0.152  | 0.161  | 0.151  | 0.149  | 0.2     |
| LOI                            | 2.11   | 1.95   | 2.28   | 1.78   | 1.81   | 2.12   |         |
| Total                          | 99.86  | 99.88  | 99.86  | 99.86  | 99.86  | 99.81  |         |
| Mg <sup>#</sup>                | 46     | 51     | 47     | 42     | 45     | 50     | 48      |
| La                             | 10.89  | 12.67  | 10.51  | 14.57  | 10.70  | 12.10  | 19.2    |
| Ce                             | 21.62  | 27.35  | 20.93  | 32.89  | 21.4   | 26.23  | 37.3    |
| Pr                             | 2.73   | 3.13   | 2.66   | 4.25   | 2.61   | 3.39   |         |
| Nd                             | 10.90  | 13.58  | 10.66  | 16.66  | 10.30  | 13.69  | 18.2    |
| Sm                             | 2.16   | 2.35   | 2.10   | 3.19   | 1.90   | 2.73   | 3.4     |
| Eu                             | 0.74   | 0.83   | 0.75   | 0.90   | 0.74   | 0.86   | 0.9     |
| Gd                             | 1.83   | 1.99   | 1.78   | 2.54   | 1.58   | 2.11   | 2.8     |
| Tb                             | 0.3    | 0.32   | 0.29   | 0.39   | 0.24   | 0.35   |         |
| Dy                             | 1.71   | 1.82   | 1.66   | 2.18   | 1.44   | 2.14   | 1.9     |
| Ho                             | 0.31   | 0.35   | 0.30   | 0.41   | 0.26   | 0.33   |         |
| Er                             | 0.89   | 1.12   | 0.85   | 1.22   | 0.78   | 0.98   | 0.96    |
| Tm                             | 0.14   | 0.18   | 0.14   | 0.21   | 0.13   | 0.14   |         |
| Yb                             | 0.91   | 1.05   | 0.89   | 1.33   | 0.82   | 0.93   | 0.88    |
| Lu                             | 0.13   | 0.18   | 0.12   | 0.19   | 0.12   | 0.16   | 0.17    |
| ΣREE                           | 55.26  | 66.89  | 53.64  | 80.93  | 53.01  | 66.35  |         |
| Y                              | 7.86   | 8.84   | 7.67   | 10.95  | 6.77   | 9.89   | 10      |
| Ba                             | 528.2  | 413.2  | 482.8  | 392.8  | 458.8  | 439.6  | 721     |
| Rb                             | 39.8   | 25.7   | 31.9   | 26.3   | 25.9   | 31.2   | 52      |
| Sr                             | 458.6  | 421.2  | 453.5  | 462.2  | 475.3  | 445.1  | 565     |
| Zr                             | 113.2  | 99.4   | 105.5  | 98.3   | 99.5   | 105.9  | 108     |
| Nb                             | 2.78   | 2.93   | 2.52   | 3.32   | 2.50   | 2.33   | 6       |
| Th                             | 4.29   | 3.73   | 3.56   | 4.43   | 3.24   | 4.35   |         |
| Ni                             | 6.20   | 5.90   | 5.40   | 6.40   | 5.20   | 6.32   | 20      |
| V                              | 90.50  | 67.50  | 83.50  | 62.20  | 74.80  | 79.43  | 95      |
| Cr                             | 11.5   | 12.3   | 9.3    | 13.9   | 9.0    | 12.4   | 41      |
| Hf                             | 7.00   | 7.52   | 9.02   | 8.76   | 6.85   | 8.64   |         |
| Sc                             | 7.88   | 6.12   | 7.45   | 6.17   | 5.96   | 7.13   |         |
| Ta                             | 0.20   | 0.23   | 0.23   | 0.29   | 0.20   | 0.19   |         |
| Co                             | 10.60  | 9.30   | 10.10  | 7.60   | 9.00   | 9.89   |         |
| Li                             | 27.12  | 21.4   | 28.93  | 19.45  | 19.44  | 25.31  |         |
| U                              | 1.04   | 0.95   | 0.19   | 0.86   | 0.99   | 0.73   |         |

注:氧化物含量%;稀土、微量元素含量 10<sup>-6</sup>;高Si埃达克岩为 267 个样品平均值(Martin et al.,2005)。

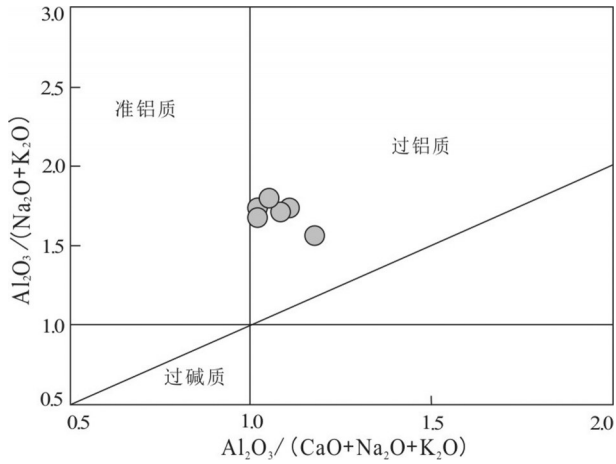


图4 额很傲包图英云闪长岩铝饱和指数(A/NK-A/CNK)图解(据 Maniar and Piccoli, 1989)  
Fig.4 Shand's index of the Ehenaoaotu tonalite (after Maniar and Piccoli, 1989)

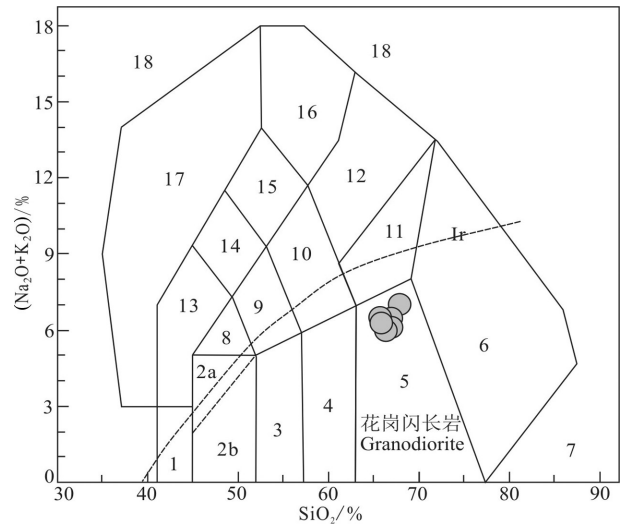


图5 额很傲包图英云闪长岩 TAS分类图(据 Middlemost,1994)  
Fig.5 Total alkalis vs. silica(TAS) classification diagram of the Ehenaoaotu tonalite (after Middlemost,1994)

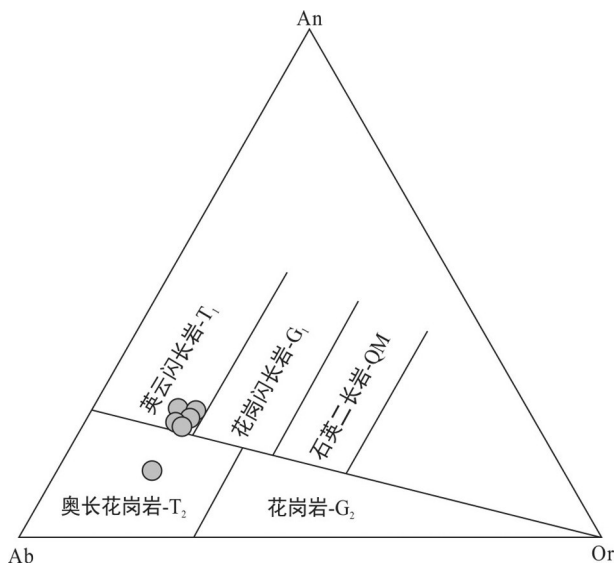


图6 额很傲包图英云闪长岩 An-Ab-Or分类图解(据 O'Connor,1965)  
Fig.6 An-Ab-Or classification diagram of the Ehenaoaotu tonalite (after O'Connor,1965)

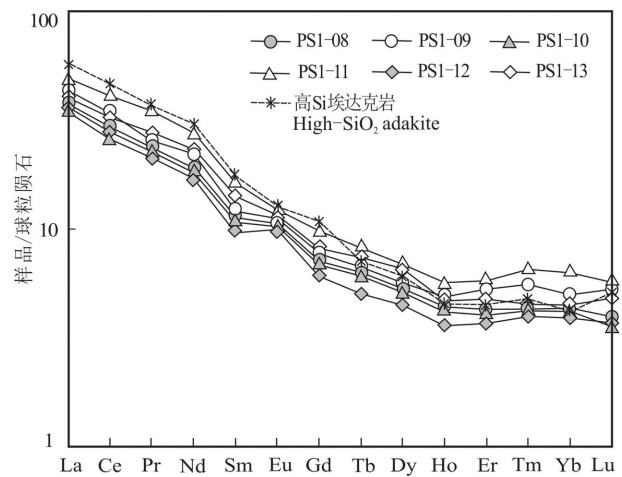


图7 额很傲包图英云闪长岩稀土元素球粒陨石标准化配分模式(球粒陨石标准化数值据 Boynton, 1984;高Si埃达克岩据 Martin et al.,2005)  
Fig.7 Chondrite-normalized REE distribution patterns of the Ehenaoaotu tonalite (normalizing values after Boynton, 1984;High-SiO<sub>2</sub> adakite after Martin et al.,2005)

$10^{-6}$ , 平均值  $0.99 \times 10^{-6}$ ; Y 含量  $6.77 \times 10^{-6} \sim 10.95 \times 10^{-6}$ , 平均值  $8.66 \times 10^{-6}$ 。该英云闪长岩的铕异常不明显,  $\delta Eu$  为 0.94~1.27, 平均值 1.11,  $(La/Yb)_N$  7.39~8.80, 轻重稀土分离明显, 球粒陨石标准化的 REE 曲线呈 LREE 富集 HREE 亏损的右倾模式(图7)。

4.3 微量元素特征

如表2所示, 该英云闪长岩具有高 Sr 和高 Sr/Y 比值的特征, Sr 含量  $421.2 \times 10^{-6} \sim 475.30 \times 10^{-6}$ , 平均

值  $452.65 \times 10^{-6}$ ; Sr/Y 比值为 42.21~70.21, 平均值 53.76。在原始地幔标准化的微量元素比值蛛网图中(图8), 具有明显的 Rb、Ba、Sr、K 正异常和 Nb、Ti、P 负异常, 与岛弧型岩浆岩微量元素分布型式相似。

5 讨论

5.1 岩石成因类型与构造环境

如前所述, 额很傲包图英云闪长岩体的  $SiO_2 >$

表3 额很傲包图英云闪长岩和高Si埃达克岩平均成分

Table 3 Average compositions of the Ehenaoaotu tonalite and high-SiO<sub>2</sub> adakites

| 岩石名称       | SiO <sub>2</sub> | Al <sub>2</sub> O <sub>3</sub> | MgO  | Na <sub>2</sub> O/K <sub>2</sub> O | Sr     | Yb   | Y     | Sr/Y  |
|------------|------------------|--------------------------------|------|------------------------------------|--------|------|-------|-------|
| 额很傲包图英云闪长岩 | 66.55            | 16.04                          | 1.65 | 2.50                               | 452.65 | 0.99 | 8.66  | 53.76 |
| 高Si埃达克岩    | 64.80            | 16.64                          | 2.18 | 2.13                               | 565.00 | 0.88 | 10.00 | 56.50 |

注:氧化物含量%,稀土、微量元素含量10<sup>-6</sup>。额很傲包图英云闪长岩为研究区6个样品平均值,高Si埃达克岩为267个样品平均值(Martin et al.,2005)。

56%, Al<sub>2</sub>O<sub>3</sub>>15%, MgO<3%, Na<sub>2</sub>O/K<sub>2</sub>O 比值>2, Sr>400×10<sup>-6</sup>, Yb<1.9×10<sup>-6</sup>, Y<18×10<sup>-6</sup>, Sr/Y 比值>40, 可与标准高Si埃达克岩相对比(表3); LREE 相对HREE 强烈富集, 无明显的Eu 异常, 并与高Si埃达克岩(267个样品平均值)的稀土配分曲线基本吻合(图7); 该岩石Rb、Ba、K 和Sr 等大离子亲石元素相对富集, Nb、P 和Ti 等高场强元素相对亏损, 与高Si埃达克岩(267个样品平均值)蛛网图曲线相吻合(图8)。这些地球化学特征与国内、外典型岛弧型埃达克岩的特征相一致(Defant et al., 1990; 刘敦一等, 2003; 王强等, 2003; Martin et al., 2005; 王金芳等, 2017a, 2018c)。因此, 通过岩石学特征和主量、稀土、微量元素与标准高Si埃达克岩的对比(表3), 并参考稀土元素配分图和微量元素蛛网图等(图7, 8), 额很傲包图英云闪长岩应归属为埃达克岩。

埃达克岩的岩浆成因和构造环境一直存在较大争议与分歧, 可概括为以下2种主要观点:(1)俯冲洋壳部分熔融上升与上覆地幔楔橄榄岩反应成因

的岛弧型埃达克岩(O型)(Defant et al., 1990; Kelemen, 1995; Yogodzinski et al., 2001; Martin et al., 2005; Viruete et al., 2007; 邓晋福等, 2010, 2015); (2)与加厚或拆沉玄武质下地壳熔融有关的埃达克岩(C型)(Sheppard et al., 2001; Hou et al., 2004; Wang et al., 2005; Xu et al., 2008)。一般认为, 两种埃达克岩的主要区别在于岛弧型埃达克岩相对富钠(邓晋福等, 2015), 而C型埃达克岩则相对富钾。研究表明, 由大洋俯冲带俯冲洋壳部分熔融形成的埃达克岩为一种特殊的岛弧型岩浆岩, 即岛弧型中酸性富钠岩浆岩, 主要为钙碱性系列, Na<sub>2</sub>O/K<sub>2</sub>O 比值相对较大, 一般认为多大于2(Defant et al., 1990; Stern et al., 1996; 张旗等, 2001; Samaniego et al., 2002; Bourdon et al., 2003; 邓晋福等, 2015)。加厚或拆沉的玄武质下地壳部分熔融产生的埃达克岩, 则主要为高钾钙碱性系列, Na<sub>2</sub>O/K<sub>2</sub>O 比值相对较小, 一般认为多在1~2, 甚至于Na<sub>2</sub>O/K<sub>2</sub>O≤1, 而且主要与造山带碰撞造山后“去根”作用或大陆板内古

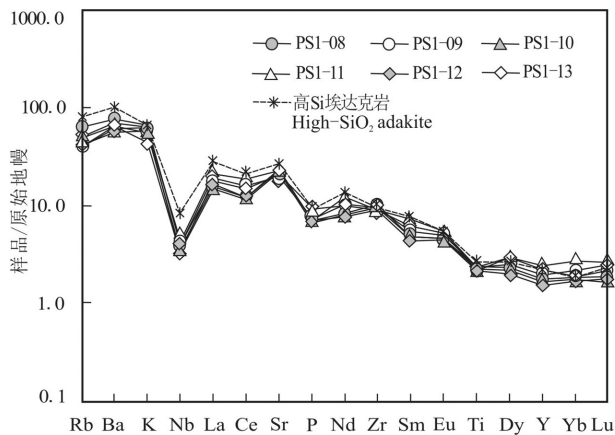


图8 额很傲包图英云闪长岩微量元素原始地幔标准化蛛网图(原始地幔标准化数值据 Sun and McDonough, 1989; 高Si埃达克岩据 Martin et al.,2005)

Fig.8 Primitive mantle-normalized trace element spider diagram of the Ehenaoaotu tonalite(normalizing values after Sun and McDonough, 1989;High-SiO<sub>2</sub> adakite after Martin et al.,2005)

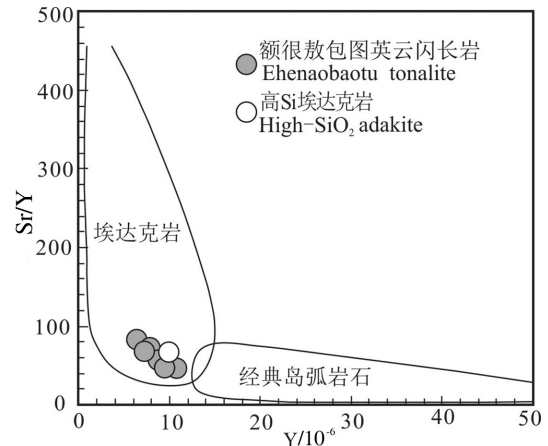


图9 额很傲包图英云闪长岩Y-Sr/Y 构造判别图解(据 Defant and Drummond,1990; Martin, 1999;高Si埃达克岩据 Martin et al.,2005)

Fig.9 Y-Sr/Y tectonic discriminant diagram of the Ehenaoaotu tonalite (after Defant and Drummond, 1990; Martin, 1999; High-SiO<sub>2</sub> adakite after Martin et al.,2005)

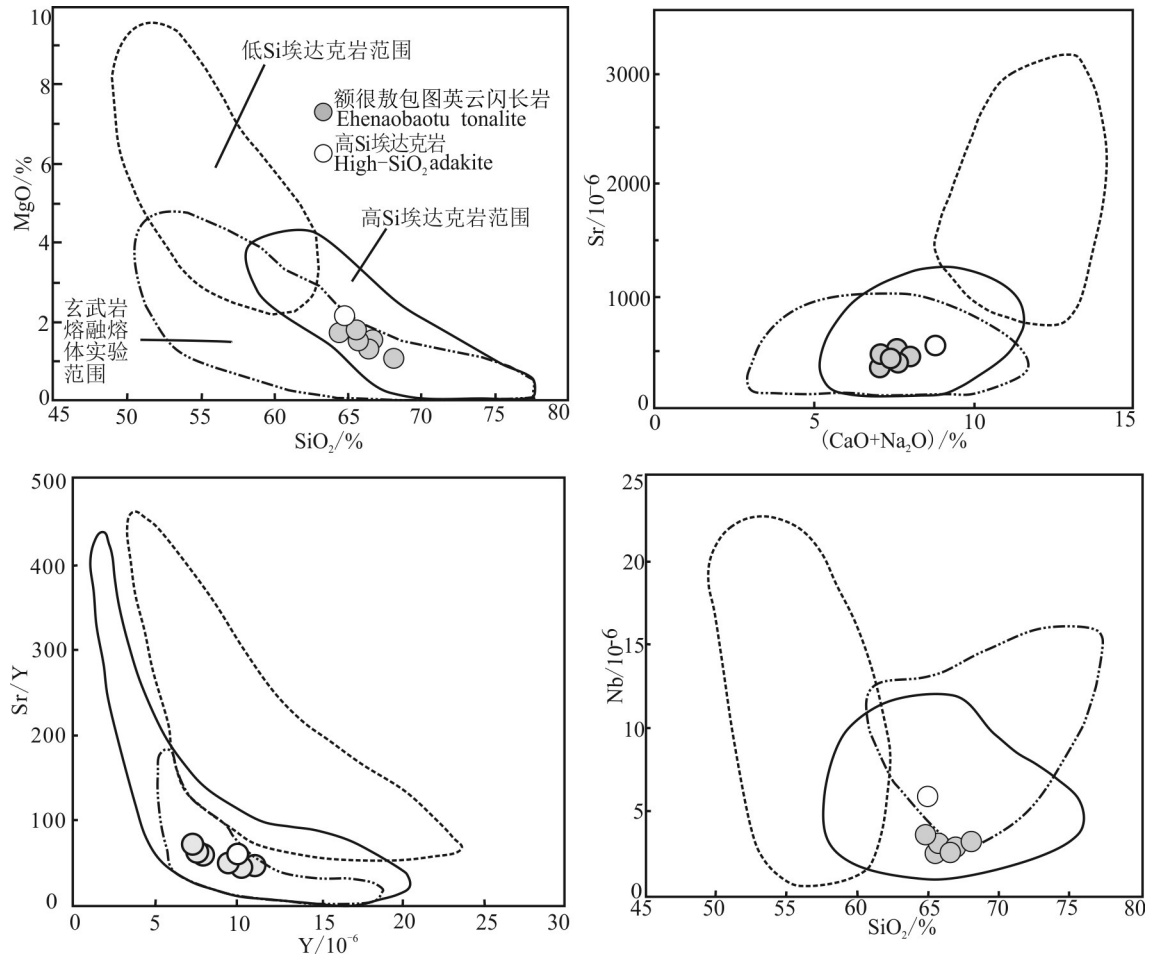


图10 额很傲包图英云闪长岩  $\text{SiO}_2$ - $\text{MgO}$ 、 $(\text{CaO}+\text{Na}_2\text{O})$ - $\text{Sr}$ 、 $\text{Y}$ - $\text{Sr}/\text{Y}$  和  $\text{SiO}_2$ - $\text{Nb}$  图解(据 Martin et al.,2005)

Fig.10  $\text{SiO}_2$ - $\text{MgO}$ 、 $(\text{CaO}+\text{Na}_2\text{O})$ - $\text{Sr}$ 、 $\text{Y}$ - $\text{Sr}/\text{Y}$  and  $\text{SiO}_2$ - $\text{Nb}$  diagrams of the Ehenaoabaotu tonalite( after Martin et al.,2005)

老克拉通的“减薄”作用有关(张旗等,2001;王强等,2003)。

本区英云闪长岩属于中钾钙碱性系列,岩石富钠贫钾,  $\text{Na}_2\text{O}/\text{K}_2\text{O}$  为 2.23~2.98, 平均值 2.5(表 3), 明显为富钠质岩石, 具有岛弧型埃达克岩相对富钠的特征。在  $\text{Y}$ - $\text{Sr}/\text{Y}$  图解中(图 9), 额很傲包图英云闪长岩均落入埃达克岩范围内, 并与岛弧型高 Si 埃达克岩(267 个样品的平均值) 投点相吻合。在  $\text{SiO}_2$ - $\text{MgO}$ 、 $(\text{CaO}+\text{Na}_2\text{O})$ - $\text{Sr}$ 、 $\text{Y}$ - $\text{Sr}/\text{Y}$  和  $\text{SiO}_2$ - $\text{Nb}$  图解中(图 10), 该岩石均落入高 Si 埃达克岩范围内, 而且总体位于玄武岩熔融熔体实验范围内。这些地球化学图解, 反映该英云闪长岩的物质来源或源区与俯冲洋壳玄武岩部分熔融物质的亲缘性和与岛弧型高 Si 埃达克岩源区的相似性, 表明该英云闪长岩可能为岛弧型高 Si 埃达克岩。

在  $\text{Rb}$ - $(\text{Y}+\text{Nb})$  和  $\text{Rb}$ - $(\text{Yb}+\text{Ta})$  构造环境判别图

解上(图 11), 额很傲包图英云闪长岩落在火山岛弧范围内, 反映其为岛弧环境产物(Thorkelson et al., 2005; Viruete et al., 2007)。在识别 TTG 岩类(英云闪长岩-奥长花岗岩-花岗闪长岩)的  $\text{An}$ - $\text{Ab}$ - $\text{Or}$  分类图解中(图 6), 额很傲包图英云闪长岩体有 4 个样品投在英云闪长岩  $\text{T}_1$ (tonalite) 区, 1 个样品投在奥长花岗岩  $\text{T}_2$ (trondhjemite) 区, 1 个样品投在英云闪长岩  $\text{T}_1$  与奥长花岗岩  $\text{T}_2$  过渡区, 反映该岩体具有  $\text{T}_1\text{T}_2\text{G}$  岩类的  $\text{T}_1\text{T}_2$  岩石组合特征(英云闪长岩-奥长花岗岩), 进一步佐证其形成于大洋岛弧环境(邓晋福等, 2015)。

综上所述, 本区英云闪长岩的形成与大洋俯冲带环境形成的岛弧型高 Si 埃达克岩相类似, 可能为俯冲洋壳部分熔融上升与上覆地幔楔橄榄岩反应成因(Rapp et al., 1999; 邓晋福等, 2015; 肖庆辉等, 2016)。然而, 与高 Si 埃达克岩相类比, 本区埃达克



岩相对富硅和明显高于 MORB 的 Th 含量(平均值  $3.93 \times 10^{-6}$ ), 以及较高的 Th/La(0.29~0.39)、Th/Sm(1.39~1.99)、Th/Yb(3.33~4.71)和 Th/Ce(0.13~0.20) 比值, 又反映本区埃达克岩的岩浆源区除俯冲洋壳玄武岩部分熔融产生的熔体之外, 尚有大洋俯冲沉积物组分参与部分熔融产生的(富 Si)熔体。而且, 额很傲包图埃达克岩的  $Mg^\#$  平均值为 47, 大于玄武岩部分熔融实验熔体的  $Mg^\#$  值(45), 表明富 Si 熔体等板片熔体沿俯冲带向上运移过程中与上覆地幔楔橄榄岩之间发生反应, 导致初始埃达克质岩浆的  $Mg^\#$  升高 (Sajona et al., 1993; Martin et al., 2005)。因此, 大洋俯冲洋壳+俯冲沉积物部分熔融产生的初始埃达克质熔体上升与上覆地幔楔橄榄岩反应, 可能为额很傲包图埃达克岩的成因机制 (图 12) (Defant et al., 1993; Samaniego et al., 2002; Ishizuka et al., 2014; 邓晋福等, 2015; 肖庆辉等, 2016; Safonova, 2017)。

## 5.2 古亚洲洋洋内俯冲作用

中亚造山带东段二连—贺根山缝合带区域地质调查研究工作取得重要进展, 区内获得大量石炭纪蛇绿岩、石炭纪—二叠纪岛弧岩浆岩和三叠纪—早白垩世后造山 A<sub>2</sub> 型花岗岩类的岩石学和年代学成果 (图 1b) (Miao et al., 2008; Xiao et al., 2009; Chen et al., 2009; Jian et al., 2012; Liu et al., 2013; 邵济安, 2015; Zhang et al., 2015; 邓晋福等, 2015; 李英杰等, 2015, 2018b; 田树刚等, 2016; 李钢柱等,

2017; 王金芳等, 2017a, 2018b; 王树庆等, 2018), 为古亚洲洋二连—贺根山洋盆在石炭纪—中二叠世早期仍然存在和“晚二叠世”闭合提供了重要岩石学与年代学证据与约束。

Jian et al. (2012) 在贺根山蛇绿岩的辉长岩墙和斜长花岗岩脉中分别获得 354 Ma 和 333 Ma SHRIMP 锆石 U-Pb 年龄, 提出贺根山蛇绿岩形成于早石炭世。Zhang et al. (2015) 在二连浩特东蛇绿岩中获得辉长岩锆石 U-Pb 年龄为 354 Ma 和 353 Ma, 斜长花岗岩年龄为 345 Ma, 指出该蛇绿岩形成于早石炭世。李英杰等 (2016) 在迪彦庙舜来可吐 SSZ 型蛇绿岩中获得层状辉长岩 LA-ICP-MS 锆石 U-Pb 年龄为 330 Ma, 蛇绿岩形成时代为早石炭世。李英杰等 (2015) 在梅劳特乌拉 SSZ 型蛇绿岩中获得辉长岩的 LA-ICP-MS 锆石 U-Pb 年龄为  $(308.5 \pm 2.2)$  Ma, 提出该蛇绿岩形成于晚石炭世。Miao et al. (2008) 在贺根山蛇绿岩带朝克山蛇绿岩中获得辉绿岩(墙) SHRIMP 锆石 U-Pb 年龄为  $(295 \pm 9)$  Ma, 认为朝克山蛇绿岩形成于晚石炭世。李刚柱等 (2017) 在内蒙古索伦山蛇绿岩带硅质岩中发现早二叠世放射虫化石, 提出索伦山蛇绿岩形成时间持续到早二叠世, 并提出古亚洲洋闭合时间在早二叠世之后。王惠等 (2005) 在内蒙古中部达茂旗巴彦敖包地区硅质岩中发现早二叠世晚期—中二叠世早期的放射虫化石, 认为索伦山蛇绿岩带形成时间为中二叠世早期。越来越多的蛇绿岩年代学研究成果表

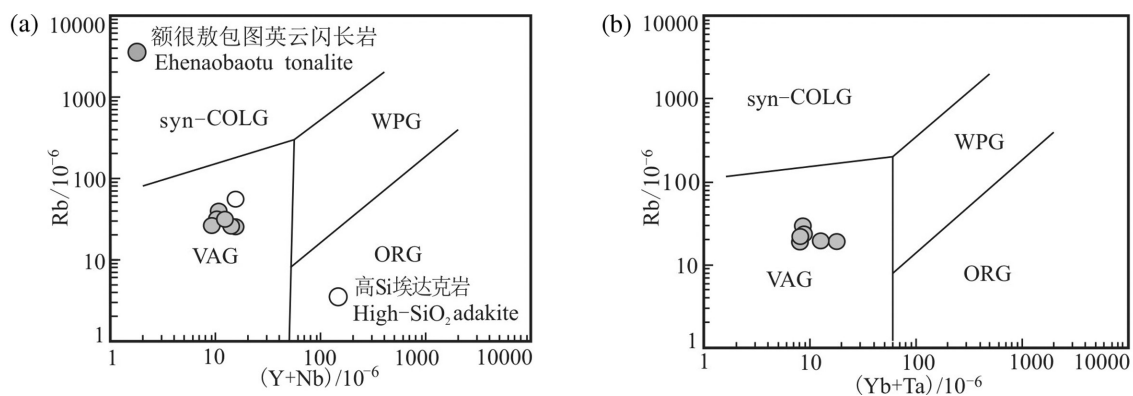


图 11 额很傲包图英云闪长岩(Y+Nb)-Rb(a)及(Yb+Ta)-Rb(b)构造判别图解(据 Pearce,1984;高Si埃达克岩据 Martin et al., 2005)

Fig.11 (Y+Nb)-Rb (a) and (Yb+Ta)-Rb (b) tectonic discriminant diagrams of the Ehenaoabaotu tonalite( after Pearce,1984; High-SiO<sub>2</sub> adakite after Martin et al.,2005)  
syn-collision granites(syn-COLG), volcanic arc granites(VAG), within plate (WPG) and normal and anomalous ocean ridge (ORG) granites

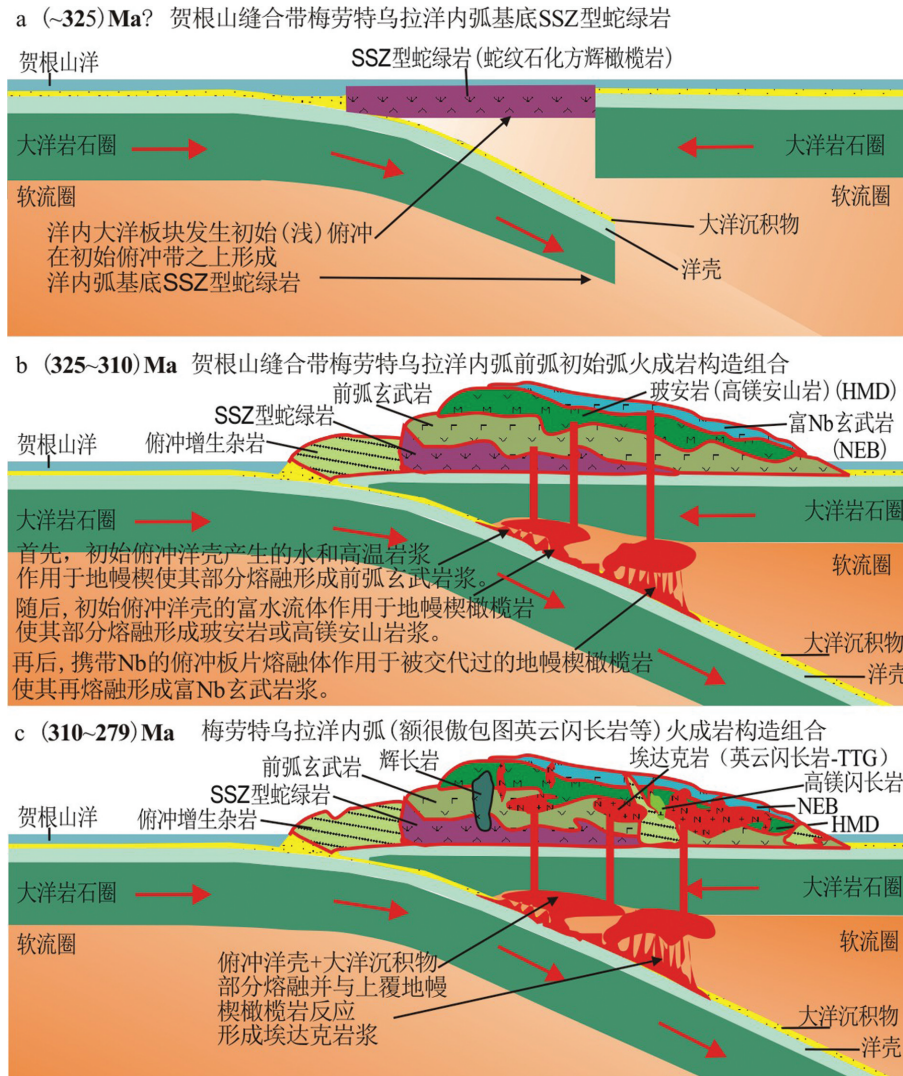


图12 额很傲包图英云闪长岩和梅劳特乌拉洋内弧火成岩构造组合成因与演化模式图

Fig.12 Genetic and evolution model of the Ehenaoabaotu tonalite and igneous petrotectonic assemblage of the Meilaotewula intra-oceanic arc

明,二连浩特—贺根山缝合带发育早石炭世—晚石炭世蛇绿岩,而且存在着早二叠世(一中二叠世早期)蛇绿岩,表明古亚洲洋二连—贺根山洋盆在石炭纪—早二叠世(一中二叠世早期)仍然存在。本文额很傲包图晚石炭世((305.6±1.5)Ma)岛弧型高Si埃达克岩或TTG岩类的识别,更进一步揭示古亚洲洋二连—贺根山洋盆在晚石炭世并没有消失,而是正处于洋壳俯冲消减阶段,晚石炭世之后的一段时间可能为古亚洲洋二连—贺根山洋盆的洋壳俯冲期。

上述蛇绿岩的形成时代与该区石炭纪—二叠纪岛弧岩浆岩的形成时代相吻合。康健丽等(2016)在锡林浩特一带早石炭世岛弧型变质基性火山岩

中获得(323~334)Ma的LA-ICP-MS锆石U-Pb年龄,提出古亚洲洋在早石炭世并没有关闭,而是正处于大洋俯冲消减阶段。刘建峰等(2009)在西乌旗南部晚石炭世早期岛弧型石英闪长岩中获得锆石LA-ICP-MS U-Pb年龄为322~325 Ma,认为形成于古亚洲洋俯冲岛弧环境。王树庆等(2018)在锡林浩特跃进地区获得一套岛弧型花岗闪长岩、英云闪长岩、石英闪长岩锆石LA-ICP-MS U-Pb年龄为310~330 Ma,提出古亚洲洋在早石炭世—晚石炭世仍然存在并处于大洋俯冲状态。刘锐等(2016)在西乌旗达青牧场和苏勒陶勒盖花岗岩中分别获得锆石LA-ICP-MS U-Pb年龄为323 Ma和

(318)Ma, 提出了晚石炭世大洋俯冲带岛弧型埃达克岩。Liu et al.(2013)在西乌旗达青牧场玄武岩中获得315~318 Ma的LA-ICP-MS锆石U-Pb年龄,认为玄武岩是晚石炭世古亚洲洋俯冲作用形成的岛弧岩浆岩。Chen et al.(2009)在白音宝力道晚石炭世岛弧型辉长闪长岩中获得SHRIMP锆石U-Pb年龄为310 Ma。张树栋等(2017)在二连浩特包饶勒敖包岛弧型石英闪长岩体中获得(302)Ma的LA-ICP-MS锆石U-Pb年龄,提出了晚石炭世末洋壳俯冲消减事件。Jian et al.(2010)在索伦山SSZ型蛇绿岩中获得洋内弧辉长岩和斜长花岗岩SHRIMP锆石U-Pb年龄分别为284 Ma和288 Ma,提出该区古亚洲洋初始俯冲时间为294~280 Ma(早二叠世)。王金芳等(2017a,2018a)在西乌旗梅劳特乌拉晚石炭世SSZ型蛇绿岩中识别出晚石炭世—早二叠世洋内弧玻安岩、埃达克岩(花岗闪长岩—英云闪长岩)和高镁闪长岩,分别获得(315.0±6.2)Ma、(294.7±1.7)Ma和(282±2)Ma的LA-ICP-MS锆石U-Pb年龄。Wang et al.(2017c)在西乌旗巴彦花识别出早二叠世岛弧型富Nb辉长岩,获得284 Ma的锆石LA-ICP-MS U-Pb年龄。总之,越来越多的岛弧岩浆岩年代学研究成果表明,二连—贺根山缝合带发育早石炭世—晚石炭世岛弧岩浆岩,存在着早二叠世岛弧岩浆岩,表明古亚洲洋二连—贺根山洋盆在石炭纪—早二叠世仍然存在。额很傲包图晚石炭世大洋俯冲带岛弧型高Si埃达克岩的确认,更进一步揭示古亚洲洋二连—贺根山洋盆在晚石炭世正处于洋壳俯冲消减过程中,而且表现出洋内俯冲作用或洋内弧(IOA intraoceanic arc)的TTG岩浆作用特征。这与该区梅劳特乌拉晚石炭世SSZ型蛇绿岩中的晚石炭世—早二叠世(315~279 Ma)洋内弧和迪彦庙SSZ型蛇绿岩中的早石炭世((333.4±8.5)Ma)达哈特洋内弧洋内俯冲与岩浆作用相一致(王金芳等,2017a,2018c,2021;李英杰等,2018b),可能反映古亚洲洋二连—贺根山洋盆在石炭纪—早二叠世存在着广泛而强烈的洋内俯冲作用,或该时期主要表现为洋内俯冲作用与洋内弧岩浆作用。

这些石炭纪—中二叠世早期蛇绿岩和岛弧岩浆岩的岩石学和年代学证据,与二连—贺根山缝合带区域内下二叠统寿山沟组半深海—深海复理石建造和中二叠统哲斯组泥岩中放射虫化石所反映

的古洋盆环境相吻合(Shang, 2004; 公繁浩等, 2013),也与该区石炭纪—早二叠世(古亚洲洋阶段)—中二叠世(兴蒙海槽阶段)构造古地理环境及演变阶段相对应(田树刚等,2016),表明古亚洲洋二连—贺根山洋盆在晚石炭世—中二叠世并没有关闭,而是正处于大洋俯冲消减阶段,大洋最终闭合应在中二叠世之后。结合二连—贺根山缝合带三叠纪—早白垩世后山造A<sub>2</sub>型花岗岩类时空分布(张晓晖等,2006;石玉若等,2007;程天赦等,2014;王金芳等,2017b,2018b,2019b,2020b,c,e),二连—贺根山缝合带碰撞造山缝合时间应为二叠纪末期。因此,本文额很傲包图晚石炭世大洋俯冲带岛弧型高Si埃达克岩的识别与确认,可能更进一步揭示了古亚洲洋二连—贺根山洋盆在石炭纪—早二叠世正处于以洋内俯冲作用为特征的大洋俯冲消亡过程,也更进一步反映了中亚造山带东段二连—贺根山缝合带在石炭纪—早二叠世可能主要通过洋内俯冲作用形成洋内弧(IOA intraoceanic arc)与大洋板块地层(OPS ocean plate stratigraphy)或俯冲增生杂岩(SAC subduction accretional complex)的洋陆转换过程与信息(李英杰等,2012,2018b;李刚柱等,2017;Li et al.,2018a;王金芳等,2019a,2020a,d,2021)。

## 6 结 论

(1)通过岩石学和岩石地球化学研究,证明了额很傲包图英云闪长岩体是岛弧型埃达克岩,其形成于大洋俯冲带岛弧环境,俯冲洋壳+俯冲深积物部分熔融产生的初始埃达克质熔体上升与上覆地幔楔橄榄岩反应可能是其成因机制。

(2)额很傲包图岛弧型埃达克岩的形成年龄为(305.6±1.5)Ma,时代为晚石炭世,表明二连—贺根山缝合带在晚石炭世存在着大洋俯冲、岛弧岩浆作用。

(3)额很傲包图晚石炭世岛弧型埃达克岩的识别与确定,及其与梅劳特乌拉晚石炭世SSZ型蛇绿岩以及区域二连—贺根山缝合带石炭纪蛇绿岩、石炭世—二叠纪岛弧型岩浆岩的时空分布与演化关系,反映古亚洲洋二连—贺根山洋盆在晚石炭世—中二叠世仍然存在,而且可能主要表现为洋内俯冲与洋内弧岩浆作用。

**致谢:**审稿专家和编辑对稿件提出了建设性的修改意见,在此表示衷心的感谢。

## References

- Altherr R, Topuz G, Sichel W. 2008. Geochemical and Sr–Nd–Pb isotopic characteristics of Paleocene plagioclites from the eastern Pontides (NE Turkey)[J]. *Lithos*, 105 (1/2):149–161.
- Bourdon E, Eissen J P, Gutscher M A. 2003. Magmatic response to early aseismic ridge subduction: The Ecuadorian margin case (South America) [J]. *EPSL*, 205:123–138.
- Boynnton W V. 1984. Geochemistry of the rare earth elements: Meteorite studies[C]//Henderson P. *Rare Earth Element Geochemistry*. Elsevier, 63–114.
- Chen B, Jahn B M, Tian W. 2009. Evolution of the Solonker suture zone constraints from U–Pb ages, Hf isotopic ratios and zircon whole–rock Nd, Sr isotope compositions of subduction– and collision–related magmas and forearc sediments[J]. *Journal of Asian Earth Sciences*, 34(3):245–257.
- Chen Bin, Zhao Guochun, Wilde Simon. 2001. Subduction and collision–related granitoids from southern Sonidzuoqi, Inner Mongolia: Isotopic ages and tectonic implications[J]. *Geological Review*, 47(4):361–367 (in Chinese with English abstract).
- Cheng Tianshel, Yang Wenjing and Wang Denghong. 2014. Zircon U–Pb age and geochemical characteristics of the Alubaoge A–type granite in Xiwuqi, Inner Mongolia and its geological significance[J]. *Geotectonica et Metallogenia*, 38(3): 718–728(in Chinese with English abstract).
- Corfu F, Hancher J M, Hoskin P W O. 2003. Atlas of zircon textures[J]. *Reviews in Mineralogy & Geochemistry*, 53(1):469–500.
- Defant J D. 1993. Mount St. Helens; potential example of the partial melting of the subducted lithosphere in a volcanic arc[J]. *Geology*, 21:547–550.
- Defant M J, Drummond M S. 1990. Derivation of some modern arc magmas by melting of young subducted lithosphere[J]. *Nature*, 347 (18):662–665.
- Deng Jinfu, Feng Yanfang, Di Yongjun, Liu Cui, Xiao Qinghui, Su Shangguo, Zhao Guochun, Meng Fei, Ma Shuai, Yao Tu. 2015. Magmatic arc and ocean–continent transition: Discussion[J]. *Geological Review*, 61(3): 473–484 (in Chinese with English abstract).
- Deng Jinfu, Liu Cui, Feng Yanfang, Xiao Qinghui, Su Shangguo, Zhao Guochun, Kong Weiqiong, Cao Wenyan. 2010. High magnesian andesitic/dioritic rocks (HMA) and magnesian andesitic/dioritic rocks (MA): Two igneous rock types related to oceanic subduction[J]. *Geology in China*, 37(4): 1112–1118(in Chinese with English abstract).
- Dong Peipei, Li Yingjie, Wang Jinfang, Li Hongyang. 2020. The Early Permian adakite in the Meilaotewula ophiolite of Inner Mongolia and intra–oceanic subduction in eastern Palaeo–Asian Ocean[J]. *Geological Bulletin of China*, 39(9): 1474–1487(in Chinese with English abstract).
- Gong Fanhao, Huang Xin, Zheng Yuejuan, Chen Shuwang. 2013. Significance of the submarine fan of Lower Permian Shoushangou Formation in West Ujimqin–Qi, Inner Mongolia[J]. *Geology and Resources*. 22(6):478–483 (in Chinese with English abstract).
- Hou Z Q, Gao Y F, Qu X M. 2004. Origin of adakitic intrusives generated during mid–Miocene eastwest extension in southern Tibet[J]. *Earth Planet Sci. Lett.*, 220: 139–155.
- Ishizuka O, Tani K, Reagan M. 2014. Klzu–Bonin–Mariana forearc Crust as a modern ophiolite Analogue[J]. *Elements*, 10:115–120.
- Jian P, Kröner A, Windley B F. 2012. Carboniferous and Cretaceous mafic–ultramafic massifs in Inner Mongolia (China): A SHRIMP zircon and geochemical study of the previously presumed integral ‘Hegenshan ophiolite’[J]. *Lithos*, 142–143: 48–66.
- Jian P, Liu D, Kröner A, Windley B F, Shi Y, Zhang W. 2010. Evolution of a Permian intraoceanic arc–trench system in the Solonker suture zone, Central Asian Orogenic Belt, China and Mongolia[J]. *Lithos*, 118 (1/2): 169–190.
- Kang Jianli, Xiao Zhibin, Wang Huichu, Chu Hang, Ren Yunwei, Liu Huan, Gao Zhirui, Sun Yiwei. 2016. Late Paleozoic subduction of the Palaeo–Asian Ocean: Geochronological and geochemical evidence from the meta–basic volcanics of Xilinhot, Inner Mongolia[J]. *Acta Geologica Sinica*, 90(2): 383–397(in Chinese with English abstract).
- Kelemen P B, Hangh K, Greenem A R. 2003. One view of the geochemistry of subduction–related magmatic arcs, with an emphasis on primitive andesite and lower crust[C]//Rudnick R L. (ed.). *Treatise On Geochemistry*, 3: 593–659.
- Kelemen P B. 1995. Genesis of high Mg# andesites and the continental crust[J]. *Contributions to Mineralogy and Petrology*, 120(1):1–19.
- Li G Z, Wang Y J, Li C Y. 2017. Discovery of Early Permian radiolarian fauna in the Solon Obo ophiolite belt, Inner Mongolia and its geological significance [J]. *Chin. Sci. Bull.*, 62: 400–406 (in Chinese).
- Li Yingjie, Wang Jinfang, Li Hongyang, Dong Peipei. 2016. *Geology in Diyanmiao Inner Mongolia*[M]. Beijing: Geological Publishing House, 133–157 (in Chinese).
- Li Yingjie, Wang Jinfang, Li Hongyang. 2012. Recognition of Diyanmiao ophiolite in Xi Ujimqin Banner, Inner Mongolia[J]. *Acta Petrologica Sinica*, 28(4):1282–1290(in Chinese with English abstract).
- Li Yingjie, Wang Jinfang, Li Hongyang. 2015. Recognition of Meilaotewula ophiolite in Xi Ujimqin Banner, Inner Mongolia[J]. *Acta Petrologica Sinica*, 31(5):1461–1470(in Chinese with English abstract).

- Li Yingjie, Wang Jinfang, Wang Genhou, Dong Peipei, Li Hongyang, Hu Xiaojia. 2018a. Discovery of the plagiogranites in the Diyanmiao ophiolite, Southeastern Central Asian orogenic belt, Inner Mongolia, China and its tectonic significance[J]. *Acta Geologica Sinica(English Edition)*, 92(2): 568–585.
- Li Yingjie, Wang Jinfang, Wang Genhou, Li Hongyang, Dong Peipei. 2018b. Discovery and significance of the Dahate fore-arc basalts from Diyanmiao ophiolite in Inner Mongolia[J]. *Acta Petrologica Sinica*, 34(2):469–482(in Chinese with English abstract).
- Liu Dunyi, Jian Ping, Zhang Qi, Zhang Fuqin, Shi Yuruo, Shi Guanghai, Zhang Nuqiao, Tao Hua. 2003. SHRIMP dating of adakites in the Tulingkai ophiolite, Inner Mongolia: Evidence for the Early Paleozoic subduction[J]. *Acta Geologica Sinica*, 77(3): 317–330(in Chinese with English abstract).
- Liu J F, Li J Y, Chi X G, Qu J F, Hu Z C. 2013. A late-Carboniferous to early early-Permian subduction-accretion complex in Daqing pasture, southeastern Inner Mongolia: Evidence of northward subduction beneath the Siberian paleoplate southern margin[J]. *Lithos*, 177(2):285–296.
- Liu Jianfeng, Chi Xiaoguo, Zhang Xingzhou, Ma Zhihong, Zhao Zhi, Wang Tiefu, Hu Zhaochu, Zhao Xiuyu. 2009. Geochemical characteristic of Carboniferous quartz-diorite in the Southern Xiwuqi Area, Inner Mongolia and its tectonic significance[J]. *Acta Geologica Sinica*, 83(3):365–376(in Chinese with English abstract).
- Liu Rui, Yang Zhen, Xu Qidong, Zhang Xiao, Jun Yao ChunLiang. 2016. Zircon U-Pb ages, elemental and Sr-Nd-Pb isotopic geochemistry of the Hercynian granitoids from the southern segment of the Da Hinggan Mts.: Petrogenesis and tectonic implications[J]. *Acta Petrologica Sinica*, 32(5):1505–1528(in Chinese with English abstract).
- Ludwig K R. 2003. User's Manual for Isoplot 3.00: A Geochronological Toolkit for Microsoft Excel[M]. Berkeley CA: Berkeley Geochronology Center, Special Publication, 4:1–71.
- Maniar P D, Piccoli P M. 1989. Tectonic discrimination of granitoids[J]. *Geological Society of America Bulletin*, 101(5): 635–643.
- Martin H, Smithies R H, Rapp R, Moyen J F. 2005. An overview of adakite, tonalite-trondhjemite-granodiorite (TTG), and sanukitoid: Relationships and some implications for crustal evolution[J]. *Lithos*, 79(1/2):1–24.
- Martin H. 1999. Adakitic magmas: modern analogues of Archaean granitoids[J]. *Lithos*, 46: 411–429.
- Miao L C, Fan W M, Liu D Y, Zhang F Q, Shi Y R, Guo F. 2008. Geochronology and geochemistry of the Hegenshan ophiolite complex: Implications for late-stage tectonic evolution of the Inner Mongolia-Daxinganling Orogenic Belt, China[J]. *Journal of Asian Earth Sciences*, 32(5):348–370.
- Middlemost E A K. 1994. Naming materials in the magma/igneous rock system[J]. *Earth-Science Reviews*, 37: 215–224.
- O'Connor J T. 1965. A classification for quartz-rich igneous rocks based on feldspar ratios[J]. *U.S. Geol. Surv. Prof. Paper*, 525-B: 79–84.
- Pearce J A, Lippard S J and Roberts S. 1984. Characteristics and tectonic significance of supra-subduction zone ophiolites[C]// Kokelaar B P and Howells M F (eds.). *Marginal Basin Geology*. Geological Society of London Special Publication, 16:77–94.
- Peccerillo A, Taylor S R. 1976. Geochemistry of eocene calc-alkaline volcanic rocks from the Kastamonu Area, Northern Turkey[J]. *Contributions to Mineralogy and Petrology*, 58: 63–81.
- Rapp R P, Shimizu N, Norman M D, Applegate G S. 1999. Reaction between slab-derived melts and peridotite in the mantle wedge: Experimental constraints at 3.8 GPa[J]. *Chemical Geology*, 160(4):335–356.
- Sajona F G, and the Maury R C, Bellon H. 1993. Initiation of subduction and the generation of slab melts in western and eastern Mindanao, Philippines[J]. *Geology*, 21: 1007–1010.
- Safonova I. 2017. Juvenile versus recycled crust in the Central Asian Orogenic Belt: Implications from ocean plate stratigraphy, blueschist belts and intra-oceanic arcs[J]. *Gondwana Research*, 47: 6–27.
- Samaniego P, Martin H, Robin C. 2002. Transition from talc-alkalic to adakitic magmatism at Cayambe volcano, Ecuador; insights into slab melts and mantle wedge interactions[J]. *Geological Society of America*, 30(11): 967–970.
- Shang Q H. 2004. The discovery and significance of Permian radiolarians Northern Orogenic belt in the northern and middle Inner Mongolia[J]. *Chinese Science Bulletin*, 49:2574–2579.
- Shao Ji'an, Tian Wei, Tang Kedong, Wang You. 2015. Petrogenesis and tectonic settings of the late carboniferous high-Mg basalts of inner Mongolia[J]. *Earth Science Frontiers*, 22(5):171–181.
- Sheppard S, Griffin T J, Tyler I M, Page R W. 2001. High- and low-K granites and adakites at a Palaeoproterozoic plate boundary in northwestern Australia[J]. *Journal of the Geological Society*, 158(3): 547–560.
- Shi Y R, Liu D Y, Zhang Q, Jian P, Zhang F Q, Miao L C, Zhang L Q. 2007. SHRIMP U-Pb zircon dating of Triassic A-type granites in Sonid Zuoqi, central Inner Mongolia, China and its tectonic implications[J]. *Geological Bulletin of China*, 26(2):183–189(in Chinese with English abstract).
- Stern C R, Killian R. 1996. Role of the subducted slab, mantle wedge and continental crust in the generation of adakites from the Andean Austral Volcanic Zone[J]. *Contributions to Mineral. Petrol.*, 123:263–281.
- Sun S S, McDonough W F. 1989. Chemical and isotope systematics of

- oceanic basalts: Implications for mantle composition and processes[J]. Geological Society of London, Special Publication, 42: 313–345.
- Thorkelson D J and Breitsprecher K. 2005. Partial melting of slab window margins: genesis of adakitic and non-adakitic magmas[J]. Lithos, 79: 24–41.
- Tian Shugang, Li Zishun, Zhanu Yongsheng, Gou Yuexuan, Zhai Daxing, Wand Meng. 2016. Late Carboniferous–Permian tectono-geographical conditions and development in Eastern Inner Mongolia and adjacent areas[J]. Acta Geologica Sinica, 90(4):688–707(in Chinese with English abstract).
- Viruete J E, Contreras F, Stein C. 2007. Magmatic relationships and ages between adakites, magnesian andesites and Nb-enriched basalt-andesites from Hispaniola: record of a major change in the Caribbean island arc magma sources[J]. Lithos, 99(3–4):151–177.
- Wang Hui, Wang Yujing, Chen Zhiyong, Li Yuxi, Su Maorong, Bai Libing. 2005. Discovery of the Permian Radiolarians from the Bayanaobao area, Inner Mongolia[J]. Journal of Stratigraphy, 29(4): 368–372(in Chinese with English abstract).
- Wang Jinfang, Li Yingjie and Li Hongyang. 2017c. Zircon LA-ICP-MS U-Pb age and island-arc origin of the Bayanhua Gabbro in the Hegenshan Suture Zone, Inner Mongolia[J]. Acta Geologica Sinica(English Edition), 91(6):2316–2317.
- Wang Jinfang, Li Yingjie, Li Hongyang, Dong Peipei. 2017a. Discovery of Early Permian intra-oceanic arc adakite in the Meilaotewula ophiolite, Inner Mongolia and its evolution model[J]. Acta Geologica Sinica, 91(8):1776–1795(in Chinese with English abstract).
- Wang Jinfang, Li Yingjie, Li Hongyang, Dong Peipei. 2017b. LA-ICP-MS zircon U-Pb dating of the Nuhete Early Cretaceous A-type granite in XiUjimqin Banner of Inner Mongolia and its geological significance[J]. Geological Bulletin of China, 36(8): 1343–1358( in Chinese with English abstract).
- Wang Jinfang, Li Yingjie, Li Hongyang, Dong Peipei. 2018a. The discovery of the Early Permian high-Mg diorite in Meilaotewula SSZ ophiolite of Inner Mongolia and its intra-oceanic subduction[J]. Geology in China, 45(4): 706–719 (in Chinese with English abstract).
- Wang Jinfang, Li Yingjie, Li Hongyang, Dong Peipei. 2018b. Zircon U-Pb dating of the Shijiashan Late Jurassic–Early Cretaceous A-type granite in Xiwuqi, Inner Mongolia and its tectonic setting[J]. Geological Bulletin of China, 37(2/3):382–396( in Chinese with English abstract).
- Wang Jinfang, Li Yingjie, Li Hongyang, Dong Peipei. 2018c. Zircon U-Pb dating and tectonic setting of the Wulan'gou adakite in Inner Mongolia[J]. Geological Bulletin of China, 37(10): 1933–1943( in Chinese with English abstract).
- Wang Jinfang, Li Yingjie, Li Hongyang, Dong Peipei. 2019a. Zircon U-Pb ages and geochemical characteristics of the Baiyinhushu trondhjemite in the Hegenshan suture zone and their tectonic implications[J]. Geological Review, 65(4): 857–872 (in Chinese with English abstract).
- Wang Jinfang, Li Yingjie, Li Hongyang and Dong Peipei. 2019b. Post-orogeny of the Hegenshan suture zone: Zircon U-Pb age and geochemical constraints from volcanic rocks of the Manketouebo Formation[J]. Geological Bulletin of China, 38(9):1443–1454 (in Chinese with English abstract).
- Wang Jinfang, Li Yingjie, Li Hongyang, Dong Peipei. 2020a. Late Carboniferous intraoceanic subduction of the Paleo-Asian Ocean: New evidence from the Zagayin high-Mg andesite in the Meilaotewula SSZ ophiolite[J]. Geological Review, 66(2):289–306 (in Chinese with English abstract).
- Wang Jinfang, Li Yingjie, Li Hongyang and Dong Peipei. 2020b. Zircon U-Pb dating, geochemistry and tectonic implication of the Artala Middle Triassic A-type granite in Inner Mongolia[J]. Geological Bulletin of China, 39(1): 51–61 (in Chinese with English abstract).
- Wang Jinfang, Li Yingjie, Li Hongyang, Dong Peipei. 2020c. Discovery of Cretaceous shoshonitic volcanic rocks strata in Wulagai area, Inner Mongolia: Evidence from zircon U-Pb chronology[J]. Geology in China, 47(3): 888–889(in Chinese with English abstract).
- Wang Jinfang, Li Yingjie, Li Hongyang, Dong Peipei. 2020d. Intra-oceanic subduction of the Paleo-Asian Oceanic Slab: New evidence from the Early Carboniferous quartz diorite in the Diyanmiao ophiolite[J]. Acta Geologica Sinica(English Edition), 94(2):565–567.
- Wang Jinfang, Li Yingjie, Li Hongyang, Dong Peipei. 2020e. Paleo-Asian Ocean subducted slab breakoff and post orogenic extension: evidence from geochronology and geochemistry of volcanic rocks in the Hegenshan suture zone[J]. Acta Geologica Sinica, 94(12): 3561–3580(in Chinese with English abstract).
- Wang Jinfang, Li Yingjie, Li Hongyang, Dong Peipei. 2021a. Late Carboniferous TTG magmatic event in the Hegenshan suture zone: zircon U-Pb geochronology and geochemical constraints from the Huduge trondhjemite[J]. Acta Geologica Sinica, 95(2):396–412(in Chinese with English abstract).
- Wang Jinfang, Li Yingjie, Li Hongyang, Dong Peipei. 2021b. The Asagetu shoshonitic volcanic rocks in the Hegenshan suture: Zircon LA-ICP-MS U-Pb ages, geochemical features and its tectonic significance[J]. Geological Review, 67(2): 67030004 (in Chinese with English abstract).
- Wang Q, McDermott F, Xu J F. 2005. Cenozoic K-rich adakitic volcanic rocks in the Hohxil area, northern Tibet: Lower-crustal

- melting in an intracontinental setting[J]. *Geology*, 33: 465–468.
- Wang Qiang, Zhao Zhenghua, Bai zhenghua. 2003. Carboniferous adakites and Nb-enriched arc basaltic rocks association in the Alataw Mountains, north Xinjiang; interactions between slabmelt and mantle peridotite and implications for crustal growth[J]. *Chinese Science Bulletin*. 48(19):2108–2115(in Chinese).
- Wang Shuqing, Hu Xiaojia, Yang Zeli, Zhao Hualei, Zhang Yong, Hao Shuang, He Li. 2018. Geochronology, geochemistry, Sr–Nd–Hf isotopic characteristics and geological significance of Carboniferous Yuejin arc intrusive rocks of Xilinhot, Inner Mongolia[J]. *Earth Science*, 43(3): 1–31 (in Chinese with English abstract).
- Windley B F, Alexeiev D, Xiao W J, Krner F, Badarch G. 2007. Tectonic models for accretion of the Central Asian Orogenic Belt[J]. *Journal of the Geological Society*, 164(1):31–47.
- Wu Yuanbao, Zheng Yongfei. 2004. Genesis of zircon and its constraints on interpretation of U–Pb age[J]. *Chinese Science Bulletin*, 49 (15): 1554–1569(in Chinese).
- Xiao Qinghui, Li Tingdong, Pan Guitang. 2016. Petrologic ideas for identification of ocean–continent transition; Recognition of intra-oceanic arc and initial subduction[J]. *Geology in China*, 43(3): 721–737(in Chinese with English abstract).
- Xiao W J, Windley B F, Hao J. 2003. Accretion leading to collision and the Permian Solonker suture, Inner Mongolia, China: Termination of the central Asian orogenic belt[J]. *Tectonics*, 22 (6): 1069–1089.
- Xiao W J, Windley B F, Huang B C. 2009. End–Permian to mid–Triassic termination of the accretionary processes of the southern Altaids; implications for the geodynamic evolution, Phanerozoic continental growth, and metallogeny of Central Asia[J]. *Int. J. Earth Sci.*, 98: 1189–1217.
- Xu W L, Hergt J M, Gao S. 2008. Interaction of adakitic melt–peridotite: Implications for the high–Mg<sup>#</sup> signature of Mesozoic adakitic rocks in the eastern North China Craton[J]. *Earth and Planetary Science Letters*, 265 (1–2): 123–137.
- Yogodzinski G M, Lees J M, Churikova T G. 2001. Geochemical evidence for the melting of subducting oceanic lithosphere at plate edges[J]. *Nature*, 409(6819):500–504.
- Zhang Q, Qian Q, Wang E Q, Wang Y, Zhao T P, Hao J and Guo G J. 2001. An East China Plateau in mid–late Yanshanian Period: Implication from adakites[J]. *Chinese Journal of Geology*, 36(2): 248–255(in Chinese with English abstract).
- Zhang Shudong, bong Zhou, Zhang Mingyang, Lai Iin, Hong Wenwu, Zhou Changhong, Zhang Xuebin. 2017. LA–ICP–MS zircon U–Pb age and its tectonic significance of Baoraoleobao quartz diorite in the Eren Nur area of China Mongolia Border Region[J]. *Geological Science and Technology Information*, 36(3): 92–102 (in Chinese with English abstract).
- Zhang X H, Zhang H F, Tang Y J, Liu J M. 2006. Early Triassic A–type felsic volcanism in the Xilinhaote–Xiwuqi, central Inner Mongolia: Age, geochemistry and tectonic implications[J]. *Acta Petrologica Sinica*, 22 (11): 2769–2780(in Chinese with English abstract).
- Zhang Z C, Li K, Li J F, Tangy W H, Chen Y, Luo Z W. 2015. Geochronology and geochemistry of the eastern Erenhot ophiolitic complex: Implications for the tectonic evolution of the Inner Mongolia–Daxinganling Orogenic Belt[J]. *Journal of Asian Earth Sciences*, 97 (Part B): 279–293.

### 附中文参考文献

- 陈斌, 赵国春, Simon Wilde. 2001. 内蒙古苏尼特左旗南两类花岗岩同位素年代学及其构造意义[J]. *地质论评*, 47(4):361–367.
- 程天赦, 杨文静, 王登红. 2014. 内蒙古西乌旗阿鲁包格山 A 型花岗岩锆石 U–Pb 年龄、地球化学特征及地质意义[J]. *大地构造与成矿学*, 38(3):718–728.
- 邓晋福, 刘翠, 冯艳芳, 肖庆辉, 苏尚国, 赵国春, 孔维琼, 曹文燕. 2010. 高镁安山岩/闪长岩类(HMA)和镁安山岩/闪长岩类(MA): 与洋俯冲作用相关的两类典型的火成岩类[J]. *中国地质*, 37(04): 1112–1118.
- 邓晋福, 冯艳芳, 狄永军, 刘翠, 肖庆辉, 苏尚国, 赵国春, 孟斐, 马帅, 姚图. 2015. 岩浆弧火成岩构造组合与洋陆转换[J]. *地质论评*, 61 (3):473–484.
- 董培培, 李英杰, 王金芳, 李红阳. 2020. 内蒙古梅劳特乌拉蛇绿岩中早二叠世埃达克岩与古亚洲洋东段洋内俯冲[J]. *地质通报*, 39 (9):1474–1487.
- 公繁浩, 黄欣, 郑月娟, 陈树旺. 2013. 内蒙古西乌旗下二叠统寿山沟组海底扇的发现及意义[J]. *地质与资源*, 22(6):478–483.
- 康健丽, 肖志斌, 王惠初. 2016. 内蒙古锡林浩特早石炭世构造环境: 来自变质基性火山岩的年代学和地球化学证据[J]. *地质学报*, 90 (2):383–397.
- 李钢柱, 王玉净, 李成元. 2017. 内蒙古索伦山蛇绿岩带早二叠世放射虫动物群的发现及其地质意义[J]. *科学通报*, 62(5):400–406.
- 李英杰, 王金芳, 李红阳, 董培培. 2016. 内蒙古迪彦庙地质[M]. 北京: 地质出版社, 133–157.
- 李英杰, 王金芳, 李红阳. 2012. 内蒙古西乌旗迪彦庙蛇绿岩的识别[J]. *岩石学报*, 28(4):1282–1290.
- 李英杰, 王金芳, 李红阳. 2015. 内蒙古西乌旗梅劳特乌拉蛇绿岩的识别[J]. *岩石学报*, 31(5):1461–1470.
- 李英杰, 王金芳, 王根厚, 李红阳, 董培培. 2018b. 内蒙古迪彦庙蛇绿岩带达哈特前弧玄武岩的发现及其地质意义[J]. *岩石学报*, 34 (2):469–482.
- 刘敦一, 简平, 张旗, 张福勤, 石玉若, 施光海, 张履桥, 陶华. 2003. 内蒙古图林凯蛇绿岩中埃达克岩 SHRIMP 测年: 早古生代洋壳消滅的证据[J]. *地质学报*, 77(3):317–330.

- 刘建峰, 迟效国, 张兴洲, 马志红, 赵芝, 王铁夫, 胡兆初, 赵秀羽. 2009. 内蒙古西乌旗南部石炭纪石英闪长岩地球化学特征及其构造意义[J]. 地质学报, 83(3):365-376.
- 刘锐, 杨振, 徐启东, 张晓军, 姚春亮. 2016. 大兴安岭南段海西期花岗岩类锆石U-Pb年龄、元素和Sr-Nd-Pb同位素地球化学:岩石成因及构造意义[J]. 岩石学报, 32(5):1505-1528.
- 邵济安, 田伟, 唐克东, 王友. 2015. 内蒙古晚石炭世高镁玄武岩的成因和构造背景[J]. 地学前缘, 22(5):171-181.
- 石玉若, 刘敦一, 张旗, 简平, 张福勤, 苗来成, 张履桥. 2007. 内蒙古中部苏尼特左旗地区三叠纪A型花岗岩锆石SHRIMP U-Pb年龄及其区域构造意义[J]. 地质通报, 26(2):183-189.
- 田树刚, 李子舜, 张永生, 官月萱, 翟大兴, 王猛. 2016. 内蒙东部及邻区晚石炭世一二叠纪构造古地理环境及演变[J]. 地质学报, 90(4):688-707.
- 王惠, 王玉净, 陈志勇, 李玉玺, 苏茂荣, 白立兵. 2005. 内蒙古巴彦敖包二叠纪放射虫化石的发现[J]. 地层学杂志, 29(4):368-372.
- 王金芳, 李英杰, 李红阳, 董培培. 2018a. 内蒙古梅劳特乌拉蛇绿岩中早二叠世高镁闪长岩的发现及洋内俯冲作用[J]. 中国地质, 45(4): 707-719.
- 王金芳, 李英杰, 李红阳, 董培培. 2018b. 内蒙古西乌旗石匠山晚侏罗世—早白垩世A型花岗岩锆石U-Pb年龄及构造环境[J]. 地质通报, 37(2/3):382-396.
- 王金芳, 李英杰, 李红阳, 董培培. 2018c. 内蒙古乌兰沟埃达克岩锆石U-Pb年龄及构造环境[J]. 地质通报, 37(10): 1933-1943.
- 王金芳, 李英杰, 李红阳. 2017a. 内蒙古梅劳特乌拉蛇绿岩中埃达克岩的发现及其演化模式[J]. 地质学报, 91(8):1776-1795.
- 王金芳, 李英杰, 李红阳. 2017b. 内蒙古西乌旗努和特早白垩世A型花岗岩LA-ICP-MS锆石U-Pb年龄及其地质意义[J]. 地质通报, (8):1343-1358.
- 王金芳, 李英杰, 李红阳, 董培培. 2019a. 贺根山缝合带白音呼舒奥长花岗岩锆石U-Pb年龄、地球化学特征及构造意义[J]. 地质论评, 65(4):857-872.
- 王金芳, 李英杰, 李红阳, 董培培. 2019b. 内蒙古贺根山缝合带后造山作用——满克头鄂博组火山岩锆石U-Pb年龄和地球化学制约. 地质通报, 38(9):1443-1454.
- 王金芳, 李英杰, 李红阳, 董培培. 2020a. 古亚洲洋晚石炭世俯冲作用:梅劳特乌拉蛇绿岩中扎嘎音高镁安山岩证据[J]. 地质论评, 66(2): 289-306.
- 王金芳, 李英杰, 李红阳, 董培培. 2020b. 内蒙古阿爾塔拉中三叠世A型花岗岩锆石U-Pb年龄、地球化学特征及构造意义[J]. 地质通报, 39(01):51-61.
- 王金芳, 李英杰, 李红阳, 董培培. 2020c. 内蒙古乌拉盖地区发现白垩纪钾玄质火山岩——来自锆石年龄的证据[J]. 中国地质, 47(3): 888-889.
- 王金芳, 李英杰, 李红阳, 董培培. 2020e. 古亚洲洋俯冲板片断裂与后造山伸展:贺根山缝合带火山岩年代学和地球化学证据[J]. 地质学报, 94(12):3561-3580.
- 王金芳, 李英杰, 李红阳, 董培培. 2021a. 贺根山缝合带晚石炭世TTG岩浆事件:奥长花岗岩锆石U-Pb年龄和地球化学制约[J]. 地质学报, 95(2):396-412.
- 王金芳, 李英杰, 李红阳, 董培培. 2021b. 贺根山缝合带阿萨格图钾玄质火山岩锆石LA-ICP-MS U-Pb年龄、地球化学特征及构造意义[J]. 地质论评, 67(2): 67030004.
- 王强, 赵振华, 白正华. 2003. 新疆阿拉套山石炭纪埃达克岩、富Nb岛弧玄武质岩:板片熔体与地幔橄榄岩相互作用及地壳增生[J]. 科学通报, 48(12):1342-1349.
- 王树庆, 胡晓佳, 杨泽黎, 赵华雷, 张永, 郝爽, 何丽. 2018. 兴蒙造山带中段锡林浩特跃进地区石炭纪岛弧型侵入岩年代学、地球化学、Sr-Nd-Hf同位素特征及其地质意义[J/OL]. 地球科学: 43(3): 1-31.
- 肖庆辉, 李廷栋, 潘桂棠. 2016. 识别洋陆转换的岩石学思路——洋内弧与初始俯冲的识别[J]. 中国地质, 43(3):721-737.
- 张旗, 钱青, 王二七, 王焰, 赵太平, 郝杰, 郭光军. 2001. 燕山中晚期的中国东部高原:埃达克岩的启示[J]. 地质科学, 36(2):248-255.
- 张树栋, 龙舟, 张明洋, 来林, 洪文武, 周长红, 张学斌. 2017. 中蒙边境额仁淖尔地区包饶勒敖包石英闪长岩锆石U-Pb年龄及构造意义[J]. 地质科技情报, 36(3):92-102.
- 张晓晖, 张宏福, 汤艳杰, 刘建明. 2006. 内蒙古中部锡林浩特—西乌旗早三叠世A型酸性火山岩的地球化学特征及其地质意义[J]. 岩石学报, 22(11):2769-2780.